

Exchange coupling in semiconductor nanostructures

M.J. Calderón,¹ Belita Koiller,^{1,2} and S. Das Sarma¹

¹*Condensed Matter Theory Center, Department of Physics,
University of Maryland, College Park, MD 20742-4111*

²*Instituto de Física, Universidade Federal do Rio de Janeiro,
Caixa Postal 68528, 21941-972 Rio de Janeiro, Brazil*

(Dated: November 3, 2019)

The exchange coupling of the spins of two electrons in double well potentials in a semiconductor background is calculated within the Heitler-London (HL) approximation. Atomic and quantum dot types of confining potentials are considered, and a systematic analysis for the source of inaccuracies in the HL approach is presented. For the strongly confining coulombic atomic potentials in the H₂ molecule, the most dramatic failure occurs at very large interatomic distances, where HL predicts a triplet ground state, both in 3D and in 2D, coming from the absence of electron-electron correlation effects in this approach. For a 2D double well potential, failures are identified at relatively smaller interdot distances, and may be attributed to the less confining nature of the potential, leading to larger overlap and consequently an inadequate representation of the two-particle states written, within HL, in terms of the ground state orbital at each isolated well. We find that in the double dot case, the range of validity of HL is improved (restricted) in a related 3D (1D) model, and that results always tend to become more reliable as the interdot distance increases. Our calculated exchange coupling is of relevance to the exchange gate quantum computer architectures in semiconductors.

PACS numbers: 03.67.Lx, 85.35.Be, 73.21.La, 85.30.-z

I. INTRODUCTION

Semiconductor spin-based quantum computation emerged from theoretical proposals showing that the required universal gates¹ could be implemented through physical operations involving single electrons bound to an array of quantum dots² or to donors.³ The localized spin of each electron serves as the single qubit by virtue of the 2-level spin-dynamics, and the (electrostatic) quantum mechanical exchange coupling between the two electrons can be used to entangle the qubits through the “exchange gate”. Exchange gates rely on the familiar exchange coupling introduced in the context of effective spin Hamiltonians. The possibility of spin manipulation in artificial homopolar molecules in semiconductor materials drew attention to the electronic exchange coupling in a variety of situations. Laterally coupled quantum dots, defined through potentials generated by lithographic gates placed over a two-dimensional electron gas (2DEG) in semiconductor heterostructures, are under extensive theoretical^{4,5,6} and experimental^{7,8,9,10,11} investigation.

Accurate calculations of exchange coupling in molecules (or artificial molecules) are extremely difficult requiring numerically intensive self-consistent solutions of Hartree-Fock equations. In semiconductor nanostructures, particularly in the context of quantum computer architectures, such intensive quantum chemistry-type numerical calculations are unwarranted for several reasons. First, the parameters entering such calculations are essentially only very approximately known in semiconductor nanostructures and, therefore, extremely accurate quantitative calculations for the exchange energy in these nanostructures is not particularly meaningful. Second, the quantum chemical type exchange calculations are not particularly valid in the semiconductor environment.

One of the simplest and most successful methods for the calculation of exchange coupling in small molecules was proposed in 1927 by Heitler and London.¹² The method, originally conceived for the treatment of the H₂ molecule, provides a clear physical picture of the electronic mechanisms responsible for fundamental properties of matter such as molecular binding and magnetism.¹³ The basic assumption of the Heitler-London (HL) method is that the many-electron lowest energy wavefunctions in molecules may be written in terms of the one-electron ground-state orbitals of the isolated constituent atoms. This immediately requires that the overlap among neighboring orbitals be small, a condition not always fulfilled in real molecules. In fact, for the equilibrium interatomic distance in the H₂ molecule ($1.5 a_B$, with a_B representing the Bohr radius), the overlap is larger than 0.7, and the HL ground-state energy is overestimated by ~ 1.5 eV, while for interatomic distances $R \gtrsim 5 a_B$ the overlap becomes smaller than 0.1 and an excellent agreement is obtained between HL and the experimentally observed ground-state energy.¹⁴ The HL approximation is thus expected to be valid for $S \ll 1$, or equivalently, for well separated atoms, namely $R \gg a_B$ in the case of H₂.

A somewhat surprising anomaly of the HL method applied to H₂ is that it predicts a triplet ground-state for $R \gtrsim 50 a_B$, in contradiction with the well established result that for a spin-independent Hamiltonian and in the absence of magnetic fields, the ground-state of an even-electron system in a symmetric potential must be a singlet.¹⁵

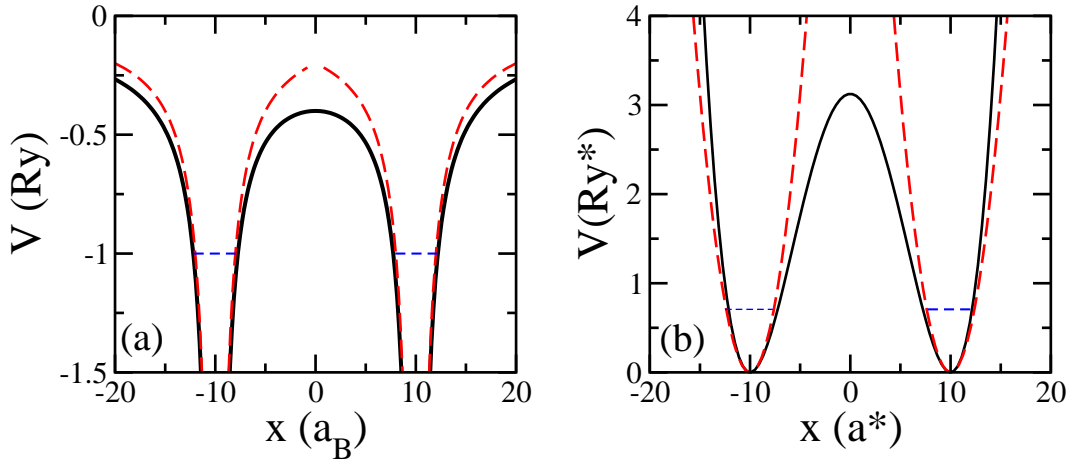


FIG. 1: (Color online) The solid lines give the profiles along the x -axis for the model potentials V considered here, while the dashed lines give the isolated-well potentials V_A and V_B . The isolated-well ground-state eigen-energy is indicated by the horizontal lines. (a) Hydrogen molecule; (b) Double-dot quartic potential from Ref. 4 [see Eq. (11)]. In this case, V_A and V_B are parabolic approximations.

Mathematically, this anomaly in HL comes from the singular nature of the Coulomb potential,¹³ leading to a logarithmic dependence of the electron-electron repulsion energy with R which becomes the dominant term at large R , resulting in a negative value of the exchange coupling $J(R) = E_{\text{triplet}} - E_{\text{singlet}}$ in this limit. Physically, this limitation may be attributed to the fact that the HL wave function is not obtained self-consistently. As compared to HL, the exact ground-state wave function incorporates correlation effects which lead to lower probability densities in regions where the electronic coordinates are near each other ($\mathbf{r}_1 \approx \mathbf{r}_2$): Of course such corrections to the singlet HL state are larger, since the triplet wavefunction already vanishes for $\mathbf{r}_1 = \mathbf{r}_2$. An asymptotically correct expression for $J(R)$ for the hydrogen molecule was obtained by Herring and Flicker,¹⁶ who have also shown that the HL results for $J(R)$ are in excellent quantitative agreement with the asymptotic expression up to R values very near the crossover to the unphysical negative range of $J(R)$.

Many calculations of exchange coupling in semiconductor quantum dots are based in the HL approximation, applied in this context to 2D model potentials. It has been pointed out that, for some parameter values of a quartic model potential proposed for the study of 2D double quantum dots, unphysical (negative) values of J are obtained within the HL approximation.⁴ This failure of HL may be due to the reduced dimensionality of the potential, since the electron-electron Coulomb interaction in 2D is expected to be larger than in 3D, or to some intrinsic limitation of this approach when applied to weakly confining gated potentials as compared to atomic-like molecular potentials. We address these questions here by considering initially the 2D hydrogen molecule, and comparing the HL results with the asymptotic expression for $J(R)$ obtained¹⁷ through a procedure analogous to the Herring and Flicker one in 3D.¹⁶ We also perform a detailed investigation of the two-electron double quantum dot quartic potential within HL, including its modified versions in 3D and 1D. The potentials considered here are plotted in Fig. 1.

We conclude that the exchange coupling obtained from the HL approach for the 2D molecular hydrogen provides reliable estimates for $J(R)$ for internuclear separations in a range comparable to the 3D case, also leading to the negative J anomaly at very large internuclear separations. We discuss the coupled double-dot within a particular 2D model potential, and we show that the unphysical negative values of J obtained here are of a different physical nature as compared to the H_2 molecule. In this case, we find that it is possible to extend the range of validity of the HL approach by considering a 3D generalized version of the model quantum dot potential, while the 1D counterpart has an even more restricted range of validity.

The H_2 molecule problem is relevant in the present context not only as a case where the HL approximation may be fully accessed by comparison to more rigorous solutions available in the literature, but also because donor-based qubits in Si rely on electronic states bound by coulombic potentials analogous to the hydrogen problem.³ The particular band structure of the Si host material brings additional complications to the exchange coupling among donor impurities¹⁸ which are not relevant in the present context. Therefore, to keep our presentation well focused, we restrict the discussions regarding coulombic potentials to the H_2 case. Of course most of our general conclusions apply to other systems by proper scaling of the Bohr radii and of the Rydberg energy to include different material properties.

This paper is organized as follows: In Sec. II we review the HL method for the H_2 molecule, and also consider the two-dimensional analogue of this problem; in Sec. III we present the HL solution for the two-electron problem in the

2D double quantum dot quartic potential introduced in Ref. 4, and also discuss its modified versions in 3D and in 1D. Further discussions and conclusions are presented in Sec. IV.

II. THE HL METHOD FOR THE H₂ MOLECULE IN 2D AND 3D

The Hamiltonian of the hydrogen molecule with nuclear coordinates \mathbf{R}_A and \mathbf{R}_B is written as¹⁴

$$H = T_1 + T_2 + V(\mathbf{r}_1) + V(\mathbf{r}_2) + \frac{e^2}{r_{12}} + \frac{e^2}{R} , \quad (1)$$

where $V(\mathbf{r}_i) = V_A(\mathbf{r}_i) + V_B(\mathbf{r}_i) = -\frac{e^2}{r_{ia}} - \frac{e^2}{r_{ib}}$, $r_{ia} = |\mathbf{r}_i - \mathbf{R}_A|$, $r_{ib} = |\mathbf{r}_i - \mathbf{R}_B|$, \mathbf{r}_i ($i = 1, 2$) are the electronic coordinates, T_i is the kinetic energy operator for electron i , $r_{12} = |\mathbf{r}_1 - \mathbf{r}_2|$ and $R = |\mathbf{R}_A - \mathbf{R}_B|$ is the inter-nuclear separation. Fig. 1(a) gives V , V_A and V_B for $\mathbf{R}_A = -\mathbf{R}_B = 10a_B\hat{x}$. Starting from normalized hydrogen atomic orbitals centered at \mathbf{R}_A and \mathbf{R}_B , which we denote for each electron i as $a(i)$ and $b(i)$, the HL lowest singlet (+) and triplet (-) 2-electron states (we omit the spin-dependent part here) are written as

$$|\pm\rangle = \frac{1}{\sqrt{2(1 \pm S^2)}} [a(1)b(2) \pm b(1)a(2)] , \quad (2)$$

with $S = \langle a(i)|b(i)\rangle$ giving the overlap integral. It is convenient to cast the exchange coupling, $J = E_{\text{triplet}} - E_{\text{singlet}} \cong \langle -|H|-\rangle - \langle +|H|+\rangle$ in the following form

$$J = \frac{2S^2}{1 - S^4} (W - C) \quad (3)$$

where

$$W = \langle a(1)b(2)|V(\mathbf{r}_1) + V(\mathbf{r}_2) - V_B(\mathbf{r}_2) - V_A(\mathbf{r}_1)|a(1)b(2) - \frac{1}{S^2}a(2)b(1)\rangle , \quad (4)$$

$$C = \langle a(1)b(2)|\frac{e^2}{r_{12}}| - a(1)b(2) + \frac{1}{S^2}a(2)b(1)\rangle . \quad (5)$$

The two terms W and C are always positive, and correspond to energy terms which contribute differently to the singlet and triplet states: W is related to the “covalent” energy, which favors the singlet state providing molecular bonding, while C is related to the electron-electron Coulomb repulsion, favoring the triplet state. Note that both terms are independent of the kinetic energy. As discussed in the introduction, physically $J > 0$, therefore we expect $W > C$.

The HL solution was presented long ago for the 3D case,¹² where an isolated atomic orbital has the form

$$a_{3D}(i) = \frac{1}{\sqrt{\pi}} e^{-r_{ia}} , \quad (6)$$

and equivalently for $b(i)$. Distances are given in units of $a_B = \hbar^2/(me^2)$. The 3D overlap is

$$S_{3D} = e^{-R} \left(1 + R + \frac{R^2}{3} \right) . \quad (7)$$

The 2D version of this problem has not been previously discussed within HL. We present it here since it is useful in addressing the effects of dimensionality, particularly regarding the electron-electron Coulomb potential. The ground-state orbital for the 2D hydrogenic atom is^{17,19}

$$a_{2D}(i) = \frac{4}{\sqrt{2\pi}} e^{-2r_{ia}} , \quad (8)$$

leading to the overlap

$$S_{2D} = 2R^2 \left(K_0(2R) + \frac{K_1(2R)}{R} \right) , \quad (9)$$

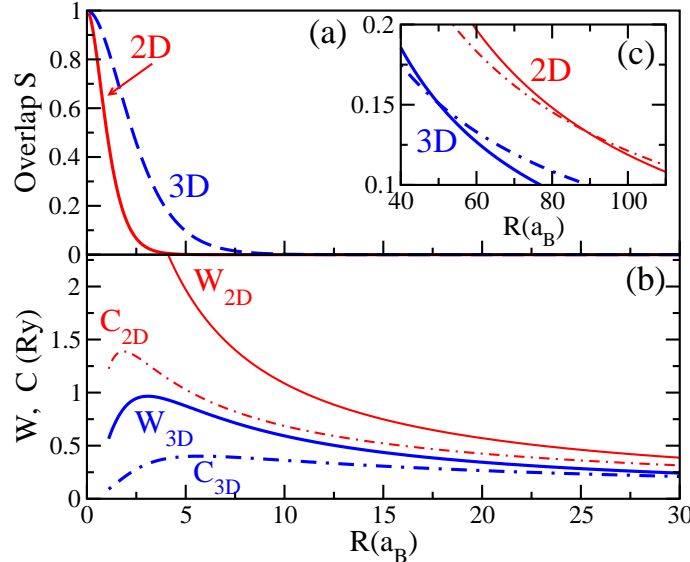


FIG. 2: (Color online) (a) Overlap between the hydrogen ground-state orbitals centered at nuclear sites a distance R apart in 2D and 3D. (b) Covalent (W) and Coulomb (C) energy terms contributing to the electronic exchange within the HL approach in the hydrogen molecule in 2D and 3D, in units of Ry . The downturn region at short distances ($R < 4$) is less reliable due to the large overlap. (c) Crossing of W and C terms at long distances. This gives the distance at which the triplet state becomes the ground-state and, therefore, Heitler-London breaks down.

where K_0 and K_1 are modified Bessel functions of the second kind. The problem in 2D is solved following the same procedure as in 3D, in particular using a 2D version of the spheroidal coordinates $\lambda = (r_a + r_b)/R$ and $\mu = (r_a - r_b)/R$, as described in detail in Ref. 14. Contrary to the 3D case, for which analytic expressions are obtained for all terms, in 2D the electron-electron Coulomb interaction terms contributing to C in Eq. (5) are obtained numerically.

In Fig. 2 we present the results for the overlap (S), the covalent energy (W), and the Coulomb energy (C), in two and three dimensions. Energies are given in units of $Ry = me^4/(2\hbar^2)$. The first thing that shows up is that, although the overlap $S_{2D}(R)$ is smaller than $S_{3D}(R)$ for all R , both W and C contributions, as well as their difference $W - C$, are larger in 2D than in 3D, which reflects the enhanced Coulomb interaction due to the electronic charge additional confinement in 2D as compared to 3D. The inset in Fig. 2 illustrates the well known artifact of HL for the 3D hydrogen problem¹⁶ giving negative $W - C$ [thus, according to Eq. (3), negative J] at very large distances (above $R \sim 50a_B$). In this inset W and C are shown to cross, with W becoming smaller than C beyond the crossing point, a behavior that also occurs in the 2D problem, where $W < C$ for very large values of R . Since for the 2D case we determine C numerically, the crossing point cannot be as precisely determined in 2D as in 3D: Within our numerical accuracy, in 2D the critical R at which J becomes negative is between 40 and $100a_B$, comparable to the 3D value. Although HL fails at long distances, the comparison of J given by Eq. (3) with the most accurate asymptotic results available in the literature for 2D and 3D,^{16,17} namely

$$\begin{aligned} J_{2D}^{\text{asymptotic}} &= 15.2R^{7/4}e^{-4R} \\ J_{3D}^{\text{asymptotic}} &= 0.8R^{5/2}e^{-2R} \end{aligned} \quad (10)$$

is very good for a wide range of distances, as shown in Fig. 3. At short distances, HL becomes less reliable due to the large overlap [see Fig. 2(a)]. Arbitrarily defining a cutoff at $S = 0.1$, we estimate the minimum distance at which we can trust the HL results to be $R_{\min}^{3D} \sim 5a_B$, and $R_{\min}^{2D} \sim 2.5a_B$, since the overlap for the 2D system decays much faster with R than for 3D.

Comparison of Figs. 2 and 3 shows that, although larger values of W , C and $W - C$ are obtained in 2D than in 3D, the opposite occurs for the exchange, with $J_{3D} \gg J_{2D}$ for all R (e.g. for $R = 10a_B$, J_{3D} is 8 orders of magnitude larger than J_{2D}). We find that the asymptotic behavior of J within HL is always dominated by the prefactor S^2 in Eq. (3) except, of course, for the change in sign discussed above.

In summary, for the H_2 molecule problem, the HL approximation provides a good estimate for the exchange coupling over a wide range of distances both in 2D and in 3D. A lower bound for R so that the HL results are reliable is given by the value of the overlap S , which must be small, while an upper bound for R is defined in this case by the physical requirement that J remains positive.

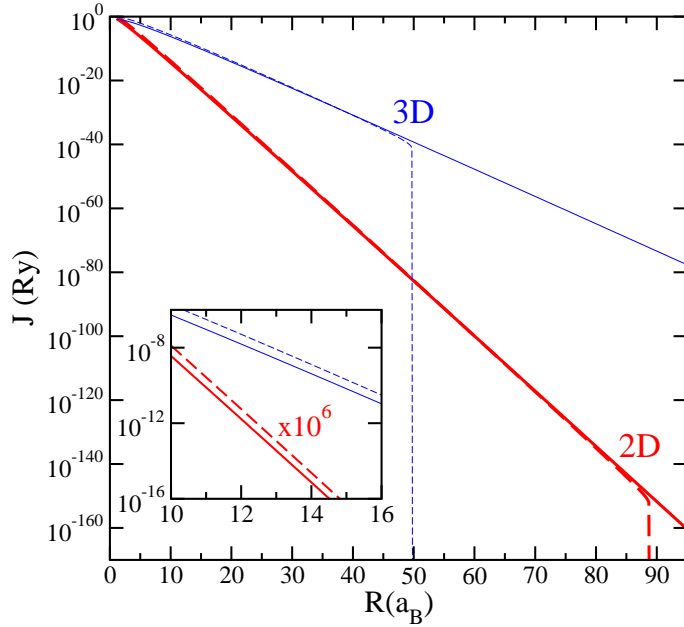


FIG. 3: (Color online) The solid lines are the asymptotic values for the electronic exchange for the hydrogen molecule in 2D and 3D, as given in Eq. (10), that we compare here with the Heitler-London results (dashed lines). The comparison is very good (see inset) up to the large distances where HL fails. The HL results are dominated by the prefactor S^2 , see Eq.(3), except for the negative- J anomaly, indicated here by the steep drop in the HL curves, which is dictated by the crossing of W and C curves in Fig. 2(c).

III. THE HL METHOD FOR THE QUARTIC DOUBLE-DOT POTENTIAL

We turn now to study exchange in quantum dots within the HL approximation. Quantum dots are defined by gate-generated potentials modifying a two-dimensional electron gas (2DEG) environment in semiconductor heterostructures. Each quantum dot is usually modeled by a harmonic well with $V_j(\mathbf{r}) = \frac{m\omega_0^2}{2}(\mathbf{r} - \mathbf{R}_j)^2$ where $\mathbf{R}_j = +R/2\hat{x}$, $-R/2\hat{x}$ for $j = A, B$ respectively. Following Burkard *et al.*⁴, the coupling of the dots in a 2D system is modeled by the quartic potential

$$V(x, y) = \frac{m\omega_0^2}{2} \left\{ \frac{\left[x^2 - \left(\frac{R}{2} \right)^2 \right]^2}{R^2} + y^2 \right\} \quad (11)$$

which satisfies $V(x \approx \pm R/2, y) = V_j(\mathbf{r})$ [see Fig. 1(b)]. The Hamiltonian for two electrons in a double quantum dot can be written as

$$H = T_1 + T_2 + V(\mathbf{r}_1) + V(\mathbf{r}_2) + \frac{e^2}{\epsilon r_{12}} \quad (12)$$

where ϵ is the semiconductor dielectric constant. For the results presented below, distances are given in units of $a^* = \hbar^2\epsilon/(m^*e^2)$ and energies in $\text{Ry}^* = m^*e^4/(2\hbar^2\epsilon^2)$, where m^* is the effective mass in the host semiconductor. Note that, contrary to the H_2 case, $V \neq V_A + V_B$. The single electron Hamiltonian is

$$h_i = T_i + V_A(\mathbf{r}_i), \quad (13)$$

the corresponding ground state orbital is $a_{2D}(i) = \frac{\beta}{\sqrt{\pi}} \exp \left\{ -\frac{\beta^2}{2} \left[(x_i \pm \frac{R}{2})^2 + y_i^2 \right] \right\}$, with $\beta = \sqrt{m\omega_0/\hbar}$, and the overlap is given by $S_{2D} = e^{-\beta^2(R/2)^2}$.

We point out that the physical significance of the covalent term W defined in Eq. (4) is somewhat different here as compared to the H_2 system. From Eq. (4), the operator involved in W is an effective potential $v = V(\mathbf{r}_1) + V(\mathbf{r}_2) - V_B(\mathbf{r}_2) - V_A(\mathbf{r}_1)$ which, for H_2 , results in $v = V_B(\mathbf{r}_1) + V_A(\mathbf{r}_2)$, related to the energy of an “ A -atom electron” due to

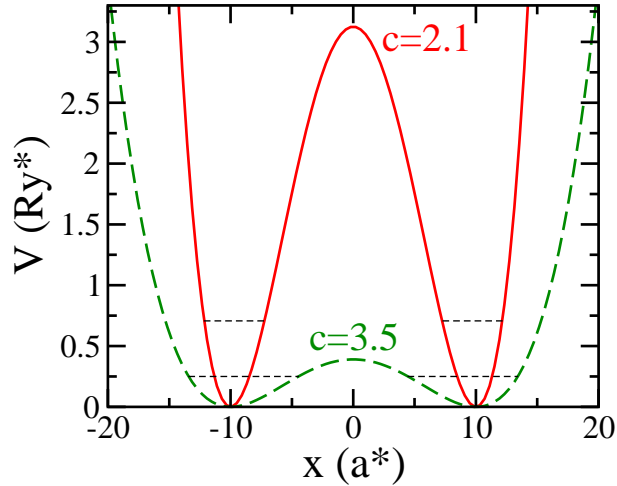


FIG. 4: (Color online) Profiles along the x -axis for the double-dot quartic potential [Eq.11], for two values of c . The horizontal lines indicate the single-well ground state energies in the harmonic approximations. As c increases, a lower barrier is obtained, and each well becomes less confining. As a consequence, the overlap increases (see text).

the potential V_B of the B -atom and vice versa. In the double quantum dot, $v \neq V_B(\mathbf{r}_1) + V_A(\mathbf{r}_2)$, instead the effective potential v involves differences between the quartic potential and quadratic terms. In this way, the “electron in the A -dot” does not “feel” the potential V_B , but an approximated version of it.

Using the expressions for W and C given in Eqs. (4) and (5) we get,⁴

$$W_{2D} = \frac{3}{4} \hbar \omega_0 \left(1 + \frac{\beta^2 R^2}{4} \right) , \quad (14)$$

and

$$C_{2D} = \hbar \omega_0 c \left(1 - e^{-\frac{\beta^2 R^2}{4}} I_0 \left(\frac{\beta^2 R^2}{4} \right) \right) \quad (15)$$

where I_0 is the modified Bessel function of the first kind and

$$c = \sqrt{\frac{\pi}{2}} \frac{e^2 \beta / \epsilon}{\hbar \omega_0} \quad (16)$$

is a parameter introduced in Ref. 4 as the ratio between the Coulomb and the confining energy. Note that c is also completely defined by ω_0 , since $\beta \sim \sqrt{\omega_0}$. Fig. 1(b) gives V , V_A and V_B for $R = 20a^*$ and $c = 2.1$. In Fig. 4 we compare the quartic potential for two values of c .

Fig. 5 shows the behavior of the overlap, W_{2D} and C_{2D} vs R for different values of c . As mentioned by Burkard *et al.*,⁴ when $c > 2.8$ the HL approach breaks down, predicting negative exchange J for certain distances R . We illustrate this behavior in Fig. 5(b)-(d) where we plot W_{2D} (solid line) and C_{2D} (dash) vs R for increasing values of c , and the lines are seen to cross when $c > 2.8$, namely frames (c) and (d). In all cases, W_{2D} increases quadratically with R , while C_{2D} also increases with R but eventually saturates towards $\hbar \omega_0 c$ as $R \rightarrow \infty$. This means that, at any fixed $R > 0$ the curves always cross for large enough c , while for large enough R , one always gets $W > C$ and thus positive J , regardless of c . This last remark means that the large- R anomaly encountered in the H_2 HL solution does not occur here.

We have argued above that the HL wave-function does not incorporate correlation effects, leading to overestimated values of the Coulomb repulsion between the electrons and eventually resulting in negative J . For the cases shown here, C_{2D} gets very close, and even crosses W_{2D} at short distances. In this small- R region, the HL approximation is not reliable because S is large [see Fig. 5 (a)], a fact that may also affect the relative values of W and C , leading to the unphysical negative- J behavior. However, for the region of larger R , one eventually gets $J > 0$ and $S \ll 1$, thus we expect the HL results for J to be reliable at large R , even for $c > 2.8$. For example, considering $c = 3.5$ and $R = 20a^*$, results in Fig. 5(c) are physically sound, as would be expected from the energy profile given in Fig. 4. For the same distance and $c = 7$, the quartic potential gives a barrier that is lower than the single particle eigenenergy,

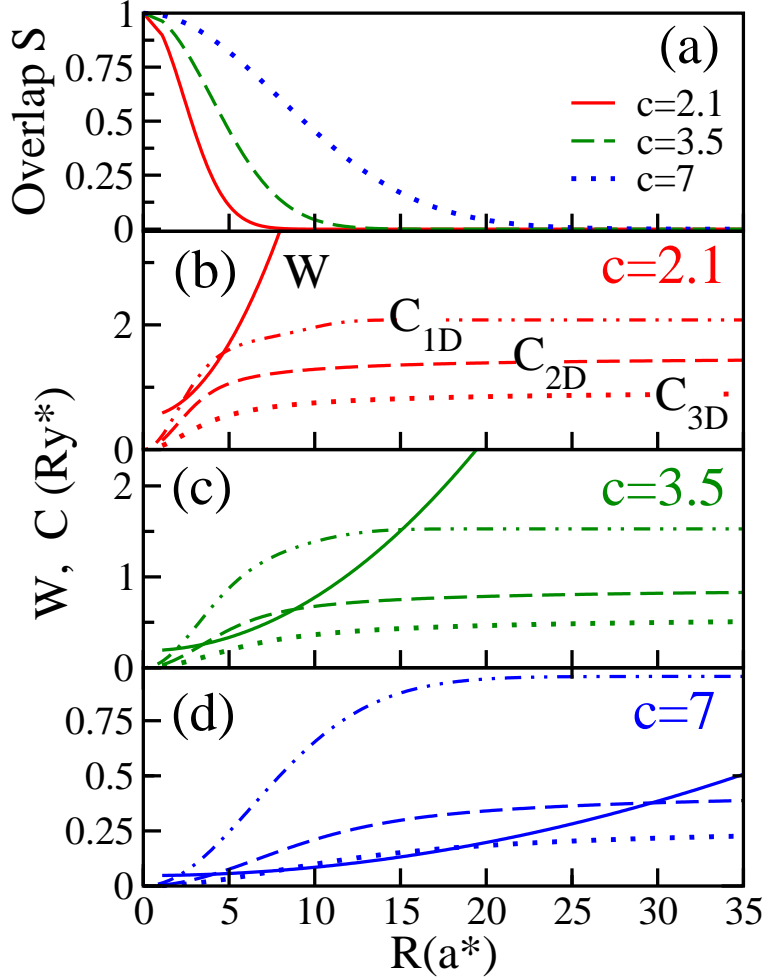


FIG. 5: (Color online) (a) Overlap for three different values of the parameter c [defined in Eq. (16)] for the double quantum dot problem. (b), (c), and (d) Covalent ($W = W_{1D} = W_{2D} = W_{3D}$) and Coulomb (C) energy terms for the double quantum dot problem in 1D, 2D, and 3D. When the overlap is large, HL results are not reliable and, for larger values of c , lead to negative exchange J .

in clear contradiction with the HL underlying assumptions: The failure of HL for $R = 20a^*$ in Fig. reffig:quartic(d) is not surprising. We point out that the barrier raises as R increases.

In order to investigate the effect of dimensionality, it is instructive to compare the two-dimensional system with a similar three-dimensional problem, as done for H_2 in Sec. II. From the 2D potential in Eq. (11), we define a 3D counterpart as $V_{3D}(x, y, z) = V(x, y) + \frac{m\omega_0^2}{2}z^2$, with the ground state orbital $a_{3D}(i) = \frac{\beta^{3/2}}{\pi^{3/4}} \exp\left\{-\beta^2 \left[\left(x_i \pm \frac{R}{2}\right)^2 + y_i^2 + z_i^2\right]/2\right\}$, leading to $S_{3D} = S_{2D}$, $W_{3D} = W_{2D}$ and

$$C_{3D} = \frac{2}{\pi} \hbar \omega_0 c \left[1 - \sqrt{\frac{\pi}{2}} \frac{\text{Erf}(\beta R/\sqrt{2})}{\beta R} \right], \quad (17)$$

where $\text{Erf}(x) = \frac{2}{\sqrt{\pi}} \int_0^x e^{-u^2} du$ is the Error Function. C_{3D} also saturates at long R , and the asymptotic value here is $\frac{2}{\pi} \hbar \omega_0 c$. It is clear from Fig. 5 that, similarly to the H_2 case, the three dimensional system has a lower Coulomb contribution (dotted line) to the exchange, extending the range of c values for which W does not cross C up to $c = 5.8$. It is also clear that for $c > 2.8$ the range of R for which $J > 0$ is always extended in 3D toward smaller R .

For completeness, we also discuss the 1D counterpart of the model potential in Eq. (11), $V_{1D}(x) = \frac{m\omega_0^2}{2} \left[x^2 - \left(\frac{R}{2}\right)^2\right]^2 / R^2$. The single-electron ground state is $a_{1D}(i) = \frac{\sqrt{\beta}}{\pi^{1/4}} \exp\left\{-\beta^2 \left(x_i \pm \frac{R}{2}\right)^2/2\right\}$, leading to

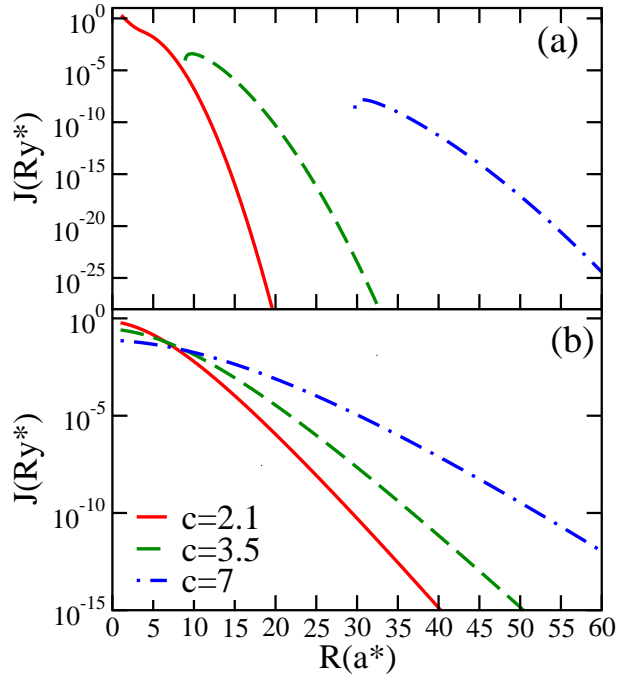


FIG. 6: (Color online) (a) Exchange at long distances R , within HL approximation, in the two-dimensional double quantum dot system, for three different values of $c = 2.1, 3.5$, and 7 . For the larger values of c , HL breaks down at small R . (b) Exchange as calculated by Ponomarev *et al.* (Eq. 44 in Ref. 19) for the same values of c .

$S_{1D} = S_{2D}$, $W_{1D} = W_{2D}$. The Coulomb term corresponds to the $\varepsilon = 0$ value of the function

$$C_{1D}(\varepsilon) = \frac{2}{\pi} \hbar \omega_0 c \left(\int_{\varepsilon}^{\infty} dx \frac{e^{-\beta^2 x^2/2}}{x} - S^2 \int_{\varepsilon}^{\infty} dx \frac{e^{-\beta^2 x^2/2} \cosh(\beta^2 Rx)}{x} \right), \quad (18)$$

where $x = |x_1 - x_2|$. In the $\varepsilon \rightarrow 0$ limit, the singular nature of the Coulomb potential in 1D systems leads to a logarithmic divergence of this expression. We overcome this problem phenomenologically by introducing a cutoff distance (the results presented in Fig. 5 correspond to $\varepsilon = 0.2a^*$) to simulate the correlation effects that would lead to a lower probability density at $x_1 = x_2$. For any chosen cutoff, the HL results in 1D are qualitatively very similar to higher dimensions. In this particular case ($\varepsilon = 0.2a^*$) the curves for C_{1D} and W cross at short distances for $c > 1.95$. The smaller the cutoff parameter ε , the larger the value of C_{1D} , and the lower the value of c that will cause HL to give a negative exchange. Strictly speaking, HL always predicts a triplet ground state for this 1D model, a characteristic that should be expected in 1D systems if electron-electron correlations are not taken into account. The singular behavior of the Coulomb potential in 1D is also responsible for the failure of HL for H_2 at large interatomic distances.

The exchange calculated from Eq. (3) for the 2D system is given in Fig. 6 (a) for the same values of c as in Fig. 5. Note that for the largest c values the curves are interrupted when J becomes negative, and for R just above this point HL predicts the equally unphysical behavior of J increasing with R .²⁰ For $c = 2.1$, J decreases monotonically with R , but the “shoulder” at $R \sim 4a^*$ is a precursor signaling this anomaly, meaning that $J > 0$ is not a sufficient condition for the reliability of the HL results. For distances far beyond these anomalous points, we find that the general behavior of $J(R)$ is dominated by the S^2 prefactor in Eq. (3). For comparison, we plot in Fig. 6(b) the exchange calculated within the Herring-Flicker approach by Ponomarev *et al.*¹⁹ for a related potential, namely the potential created by donor impurities close to a 2DEG. When a single impurity is far from the 2DEG, the electronic potential it creates may be approximated by a parabolic confinement, whose curvature defines ω_0 and thus c . The results plotted in Fig. 6(b) are obtained from Eq.(44) in Ref. 19 for distances between the donor and the 2DEG, $h = 2, 4$, and $10a^*$, respectively. We note that, beyond the anomalies cited above, the general trends in Fig. 6(a) and (b) are the same, though a detailed quantitative agreement is not found. This lack of agreement does not come as a big surprise since the exchange energy scales as S^2 . For our model, the single-electron wave-functions, and thus the overlap S and the exchange, have a gaussian decay with R , while in Ref. 19 the two-electron wave-functions have a slower exponential decay with distance.

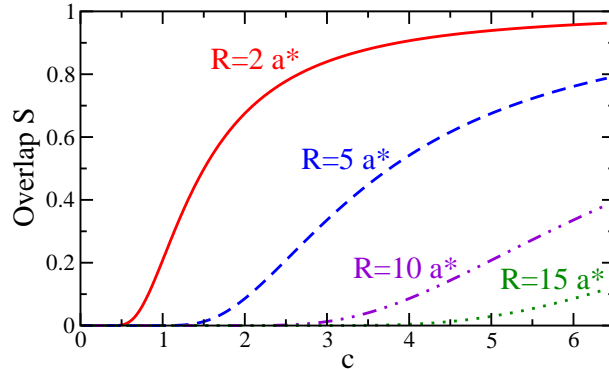


FIG. 7: (Color online) Overlap versus the parameter c defined in Eq. (16). A large parameter c corresponds to a large overlap, therefore Heitler-London breaks down. At long distances R , the overlap is small and HL gives reliable results even for larger c .

We may argue that the large- c failure of the Heitler-London approximation in this model potential is ultimately due to a large- S regime. In Fig. 7 we plot the overlap versus the parameter c defined in Eq. (16) for different values of R . We see that, for a fixed R , S increases with c (as expected from the behavior of the potential with c illustrated in Fig. 4), while it gets smaller for increasing R . Therefore, we expect HL to be reliable for any value of c given a sufficiently large interdot separation R . The values of c and R for which HL breaks down depend on the dimensionality, as shown in Fig. 5, even though S does not for this particular model.

We conclude that HL is essentially reliable for the double quantum dot problem at large enough interdot separations. This approximation breaks down for the double quantum dot quartic potential in the region of parameters where the overlap between the single electron wave-functions is large. In this region, HL is not applicable regardless of the sign of J . We have attempted a standard improvement to HL, which for the H_2 problem is to consider the Bohr radius as a variational parameter.¹⁴ In the present case this consists in taking β as a variational parameter: Although we obtain some lowering of the singlet and triplet energies by this procedure, no qualitative improvement is obtained, particularly with respect to the relative ordering of these states in regions of the parameter space where HL predicts the triplet as the ground state. The failure at long distances we encountered in the hydrogen problem is not found in the double quantum dot problem, basically due to the different nature of the confinement potential.

IV. SUMMARY AND CONCLUSIONS

The Heitler-London method¹² was originally developed for the calculation of low-lying 2-electron states in small molecules. More recently, with the development of artificial nanostructures where electrons can also be confined (quantum dots), HL proved useful as a simple tool to calculate electronic energies of low-lying states and, in particular, to estimate the exchange coupling. The basic requirement for HL to work is that the two-electron wave-functions may be written as products of the single-electron ground-state orbitals. This condition can be quantified by the overlap between the single-electron orbitals, that has to be small enough, typically $S < 0.1$. In this work, we have analyzed the reliability of HL for two types of “double-well” potentials where the individual-well confinement potential’s are of different natures: Atomic (Hydrogen atom) in Sec. II or harmonic (quantum dot) in Sec. III. There are two main differences between these problems: One refers to the strength of the confinement, much stronger in the first case as illustrated in Fig. 1, and the other to their dimensionality, 3D for atoms and 2D for quantum dots defined over a 2DEG.

For the 3D H_2 case, it has been long known¹⁶ that HL fails, namely, the triplet state is predicted to become the ground-state, when the atoms are very far apart ($R \sim 50a_B$). As argued above, at short distances HL is expected to fail as well, and it does as it overestimates the ground-state energy. We have also considered the 2D hydrogenic molecule within HL, and found qualitatively the same behavior and limitations as for the 3D H_2 case, meaning that the strongly confining atomic potential is the dominant aspect of this problem both in 3D and in 2D.

Our study of the particular quartic potential proposed by Burkard *et al.*⁴ for modeling coupled harmonic dots shows that the failure of HL at short distances is more dramatic here than in H_2 due to the less confining potential, leading to larger overlap: A triplet ground-state is predicted for a wide range of parameters. We have also pointed out the fact that the quartic potential does not correspond to the superposition of the isolated harmonic potentials as another possible source for this failure. Both effects compromise the validity of the HL representation for the low-lying states as given in Eq. (2). However, as the separation R between the dots increases, the HL method should become reliable. We

identify no failure in the long distance limit here. We have investigated the effect of dimensionality within this model potential, showing that the range of validity of HL is always extended in higher dimensions. Our main conclusion is that, although the overlap gives a quantitative hint for the validity of the HL method, other ingredients also play a role, as dimensionality and the particular form of the model potential. Reduced dimensionality overestimates the Coulomb interaction. The model potential chosen for a particular problem can affect not only the validity range of the HL method, but also the accuracy of the calculated exchange in the range of parameters when it is expected to be valid. As the exchange scales as S^2 , and S depends on the tails of the wave-function, the particular functional form chosen can change the numerical value by orders of magnitude.

Overcoming these limitations for the exchange calculation, in particular when the overlap is large, requires going beyond the HL approximation, for example increasing the basis set for the two- or many-electron wave-functions to incorporate a set of excited one-electron states. Different methods have been adopted in the literature: Molecular orbital,^{5,6} configuration-interaction,²¹ and exact diagonalization techniques.²² Also, spin polarized LDA-type calculations can be done to obtain the exchange energy,²³ but it is difficult to estimate the reliability of such theories in the present scenario. Unfortunately none of the cited methods has the conceptual and computational simplicity of HL, which should be always attempted as a first approximation in modeling new systems.

Acknowledgments

This work is supported by LPS and NSA. BK also acknowledges support by CNPq and FAPERJ.

-
- ¹ A. Barenco, C. H. Bennett, R. Cleve, D. P. DiVincenzo, N. Margolus, P. Shor, T. Sleator, J. A. Smolin, and H. Weinfurter, Phys. Rev. A **52**, 3457 (1995).
- ² D. Loss and D. P. DiVincenzo, Phys. Rev. A **57**, 120 (1998).
- ³ B. E. Kane, Nature **393**, 133 (1998).
- ⁴ G. Burkard, D. Loss, and D. P. DiVincenzo, Phys. Rev. B **59**, 2070 (1999).
- ⁵ X. Hu and S. Das Sarma, Phys. Rev. A **61**, 062301 (2000).
- ⁶ R. de Sousa, X. Hu, and S. Das Sarma, Phys. Rev. A **64**, 042307 (2001).
- ⁷ S. Tarucha, D. G. Austing, T. Honda, R. van de Hage, and L. Kouwenhoven, Phys. Rev. Lett. **77**, 3613 (1996).
- ⁸ L. Kouwenhoven, T. Oosterkamp, M. Danoesastro, M. Eto, D. G. Austing, T. Honda, and S. Tarucha, Science **278**, 1788 (1997).
- ⁹ J. R. Petta, A. C. Johnson, J. M. Taylor, E. A. Laird, A. Yacoby, M. D. Lukin, C. M. Marcus, M. P. Hanson, and A. C. Gossard, Science **309**, 2180 (2005).
- ¹⁰ A. C. Johnson, J. R. Petta, J. M. Taylor, A. Yacoby, M. D. Lukin, C. M. Marcus, M. P. Hanson, and A. C. Gossard, Nature **435**, 925 (2005).
- ¹¹ J. Gorman, D. G. Hasko, and D. A. Williams, Phys. Rev. Lett. **95**, 090502 (2005).
- ¹² W. Heitler and F. London, Z. Physik **44**, 455 (1927).
- ¹³ C. Herring, Rev. Mod. Phys. **34**, 631 (1962).
- ¹⁴ J. C. Slater, *Quantum Theory of Molecules and Solids*, vol. 1 (McGraw-Hill, New York, 1963).
- ¹⁵ E. Lieb and D. Mattis, Phys. Rev. **125**, 164 (1962).
- ¹⁶ C. Herring and M. Flicker, Phys. Rev. **134**, A362 (1964).
- ¹⁷ I. Ponomarev, V. Flambaum, and A. L. Efros, Phys. Rev. B **60**, 5485 (1999).
- ¹⁸ B. Koiller, X. Hu, and S. Das Sarma, Phys. Rev. Lett. **88**, 027903 (2002).
- ¹⁹ I. Ponomarev, V. Flambaum, and A. L. Efros, Phys. Rev. B **60**, 15848 (1999).
- ²⁰ Band interference effects, which are not relevant here, may lead locally to this behavior as obtained in Ref. 18.
- ²¹ X. Hu and S. Das Sarma, Phys. Rev. A **64**, 042312 (2001).
- ²² V. W. Scarola and S. Das Sarma, Phys. Rev. A **71**, 032340 (2005).
- ²³ V. I. Anisimov, A. E. Bedin, M. A. Korotin, G. Santoro, S. Scandolo, and E. Tosatti, Phys. Rev. B **61**, 1752 (2000).